FATIGUE BEHAVIOR AND LIFE PREDICTION OF WELDED TITANIUM ALLOY JOINTS

Jianzhong LIU, Lifa WANG and Xue-Ren WU
Beijing Institute of Aeronautical Materials, P. O. Box 81, Beijing 100095, P. R. China

Keywords: *Welded titanium alloy joints, Fatigue, Crack growth, Life prediction*

Abstract

Experimental and analytical studies were conducted on fatigue and crack growth behavior, and life prediction of both electron-beam and argon-arc welded titanium alloy (TA15) joints. For argon-arc welded titanium alloy, tests were also conducted to study the crack growth behavior of different welded areas (i.e., welded zone, heat affected zone (HAZ) and parent metal zone), and fatigue and crack growth behavior under two temperatures and three types of corrosive environments.

A small crack methodology based on the plasticity-induced crack-closure concept and the effective stress intensity factor range, ΔK_{eff}, was used to predict total fatigue lives of titanium alloy weld joints, and to simulate the effect of size and location of weld defect on fatigue lives of both electron-beam and argon-arc welds. The predicted results agreed well with experimental data.

1 Introduction

Welded titanium alloy structures are widely used in modern flight vehicles for weight and cost saving purposes. One of the concerns with welded structures, however, is the tendency of cracking and the consequent reduction of their fatigue lives. To safeguard the structural reliability, it is very important to get a good understanding of fatigue and damage tolerance behavior, and more importantly, to develop reliable methods for total fatigue life prediction of welded structures.

Titanium alloy (TA15) joints made by different weld processes are being widely used in the modern aircraft. So far, few study on fatigue and crack growth behavior of the titanium joints, especially total fatigue life prediction, has been reported [1-2].

In this paper, experimental and analytical studies were conducted on fatigue and crack growth behavior, and life prediction of both electron-beam and argon-arc welded titanium alloy (TA15) joints.

2 Material, Weld Joints and Testing Conditions

The TA15 titanium alloy sheets with a thickness of 2.5mm, were joined by electron-beam or argon-arc weld processes. The welded sheets were annealed for removing residual stresses. The tensile properties of TA15 sheet and weld zone are shown in Table 1.

Table 1 Tensile properties of TA15 sheet and weld zone

Material	σ_b [Mpa]	$\sigma_{0.2}$ [Mpa]	δ_5 (%)
TA15 sheet	1018.8	925	15.3
Electron-beam weld zone	1055		10.2
Argon-arc weld zone	979		5.47

The welded joints were made using these welded sheets, as show in Fig. 1. The weld is located at the specimen center section, the width of welded zone being about 1~2mm for electron-beam welds, and about 5~8mm for argon-arc welds.

Metallurgical analyses were made on the weld joints. Both the electron-beam and argon-arc weld joints are composed of the weld zone, the heat-affected-zone (HAZ) and the parent metal (TA15). For electron-beam weld, the

microstructures of different welded areas are given in Fig. 2. The width of HAZ is rather small, typically in the range of 0.3~1mm for electron-beam welds and 03~1.5mm for argon-arc welds. The microstructures of the three areas are significantly different, the grain sizes being the largest in the HAZ. Microhardness for the three zones was also tested. The results showed that the average of microhardnesses in the HAZ is the lowest. Therefore, one may expect that the HAZ, the fusion part, is the weakest area.

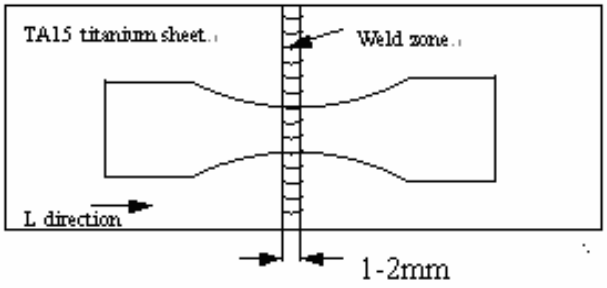

Fig. 1 Weld joint for fatigue tests

In order to study effect of weld process on fatigue properties of the weld joints, high cycle fatigue tests were carried out at three stress ratios, R=0.5, 0.06 and -1 under room temperature in air. For argon-arc welded joint, fatigue and crack growth rate tests were also conducted under two temperatures (room temperature and 250°C) and three types of corrosive environment in order to get effect of temperature and corrosive environment on fatigue and crack growth behavior of the welded joint. In addition, some tests were also performed to study the crack growth behavior of different welded areas (i.e., welded zone, HAZ and parent metal zone). The M(T) specimen is adopted in the crack growth rate experiments. Because the width of HAZ is rather small, it is not easy to obtain the crack growth data in the HAZ. The crack-starting notch at the HAZ is made about 0.15 mm above the weld line, as shown in Fig.3

The three kinds of corrosive testing environment are wet atmosphere with more than 90% relative humidity, salt fog, and salt fog+SO_2, respectively. A small sealed plastic chamber was used for corrosion fatigue experiments. During the tests, the salt fog or salt fog+SO_2 are fed continuously in the chamber by a spray system to spray, respectively a 3.5% solution of NaCl in deionized water and a solution composed of 3.5% NaCl, SO_2 with 8.7mg/m^3 and deionized water. The PH value of the salt solutions is in the range of 6.5 to 7.2.The fog and drops of the solutions, which fall out of the chamber are not returned to the solution reservoir for respraying. The spray system can keep volume of salt solutions collected in 1~2ml/(h.80cm^2) in the chamber.

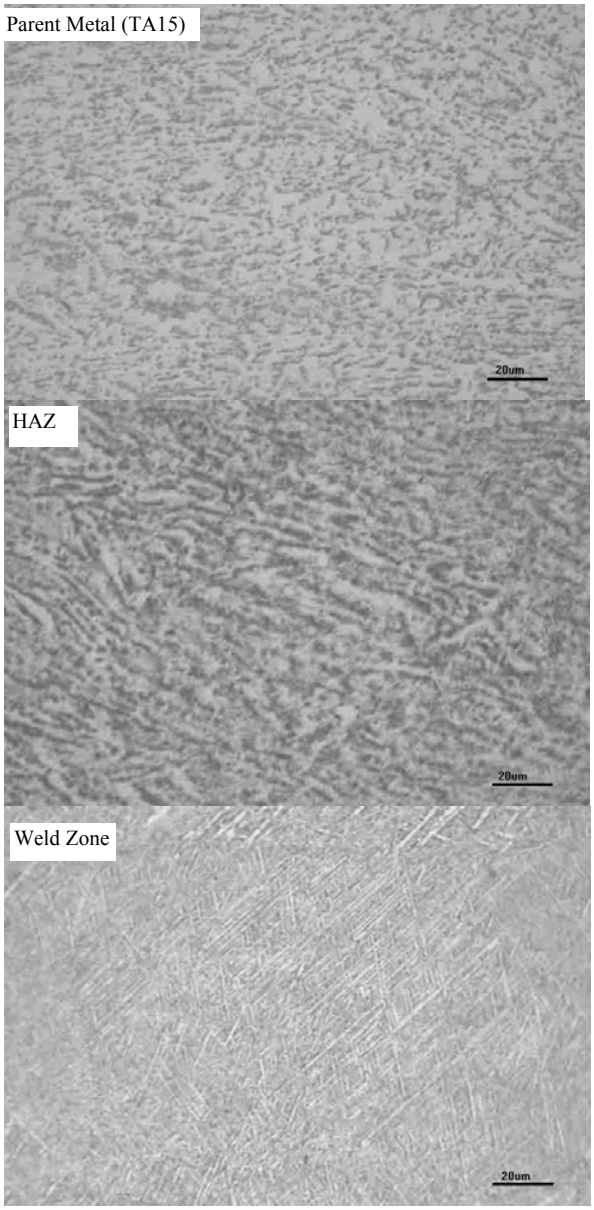

Fig. 2 Microstructures of electron-beam weld joint

All corrosion fatigue specimens were immersed in the full test environment for 24h immediately prior to testing. During experiments, the testing section of the fatigue specimen was continuously

immersed in the chamber with the corresponding corrosive environment.

For corrosion fatigue, a 50KN capacity MTS servo-hydraulic testing system was used to generate all the fatigue data. The loading waveform is sinusoidal with a frequency of 10Hz. For the fatigue testing at room temperature and 250°C in air, the AMSELER testing machine was used with a loading frequency about 80 Hz.

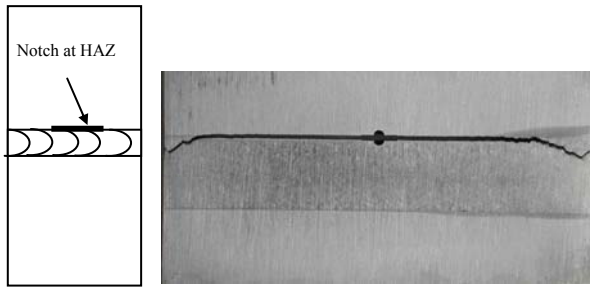

(a) (b)

Fig.3 (a) The notch on M(T) specimens, and (b) Etching picture of crack growth at the HAZ

3 Testing and Analytical Results

3.1 Fatigue Crack Initiation

Through microscopic observation and statistical analysis of the fracture of tested joints, it was found that most of the fatigue cracks initiates at weld defects (porosities) in the HAZ and at the edge of the weld. Nearly two-thirds of the specimens fractured near the HAZ, showing that the HAZ is the weakest position in the weld joints, which is in accordance with the metallographic analysis. Statistics results of crack initiation sites are given in Table 2. Figure 4 shows typical of SEM fractographic graphs concerning with crack initiation site.

Table 2 Statistics of crack initiation sites

Crack initiation sites	Electron-beam welds		Argon-arc welds	
	Number	Percent	Number	Percent
TA15 sheet	17	21.2%	1	4.4%
Weld zone	4	5%	7	30.4%
HAZ	59	73.8%	15	65.2%

3.2 Effect of Weld Process on Fatigue Properties

The effect of weld process on fatigue properties of the weld joints was studied. Test results showed that the fatigue properties of the parent metal are superior to those of the weld joints under the two weld processes at positive load ratios, as shown in Fig.5. An opposite tendency was found at negative load ratio. Fatigue properties of weld joints with different weld process do not show obvious difference, especially at or near fatigue limit.

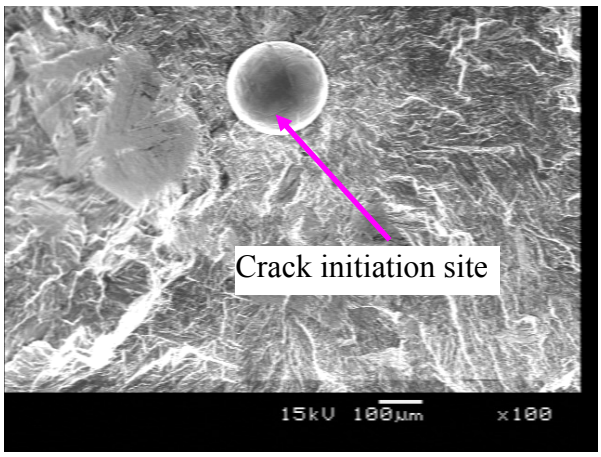

(a)

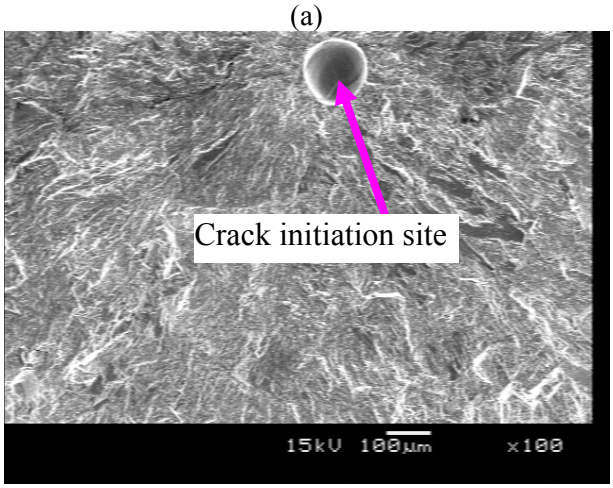

(b)

Fig.4 Typical SEM pictures of fatigue crack initiation at R=0.06， σ_{max}=600MPa; (a) argon-arc weld, (b) electron-beam weld

3.3 Effect of Experiment Temperature on Fatigue and Crack Growth Properties

Effect of temperature on both fatigue and crack growth properties of argon-arc welded joint was studied as well. The fatigue testing results are given in Fig.6. It can be found from the figure

that the effect of temperature effect on fatigue properties be quite obvious. As the temperature gets higher, the fatigue property of welded joint becomes worse. Effect of temperature on large crack growth rates of the weld zone at R=0.06 is shown in Fig.7. It is obvious that the large crack growth rates at 250ºC are almost the same as those at room temperature. Therefore, for the welded zone, the effect of temperature on large crack growth rate can be considered to be negligible. The same trend was also obtained at R=0.5.

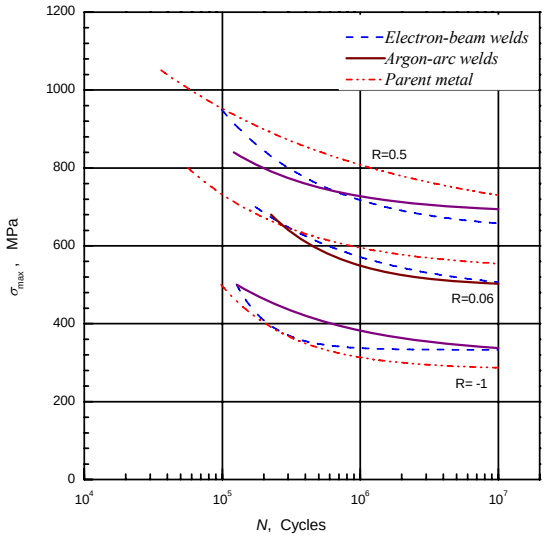

Fig.5 Comparison of the median fatigue lives among parent metal，electron-beam and argon-arc welded joints

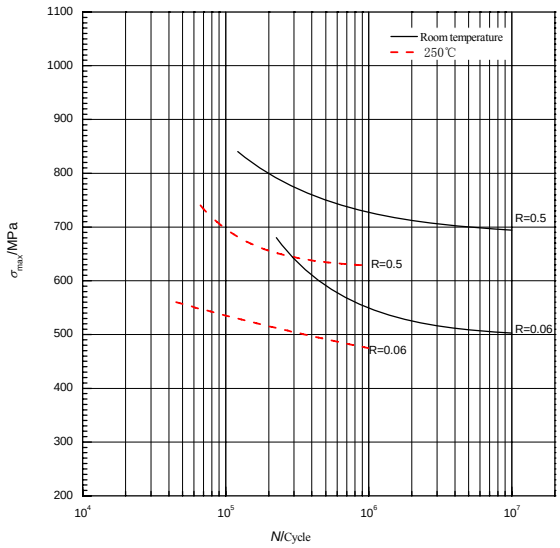

Fig.6 Comparison between median fatigue S-N curves of argon-arc welded joints at two kinds of testing temperatures

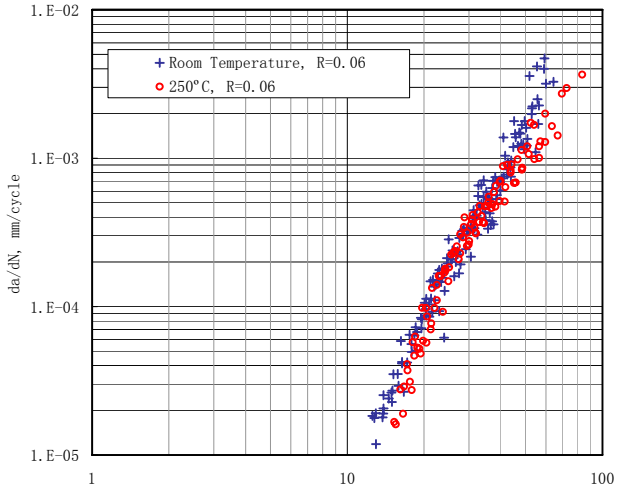

ΔK， MPa$\sqrt{m}$

Fig.7 Comparison between large crack growth rates at different temperatures for the welded zone of argon-arc welded joint

3.4 Effect of Corrosive Environment on Fatigue Properties

Figure 8 shows effect of corrosive environment on fatigue properties of argon-arc welded joint at two loading stress ratios. It can be found that the fatigue properties of welded joint in corrosive environments become worse. Among three kinds of corrosive environment, the effect of the salt fog+SO_2 is the most preeminent. Compared with the results of parent specimens, it can be found that the corrosive environment with the most preeminent effect is the same. However, the effect of the corrosive environment on the fatigue property of welded joint seems to be more obvious than that of parent material.

3.5 Crack Growth Properties at Different Welded Areas

Figure 9 gives the large crack da/dN -$\triangle K$ data for the parent TA15 metal, the weld zone and the HAZ of argon-arc joint at two loading stresses. Evidently, the large crack growth rates are higher for cracks in the HAZ than those of both the weld zone and TA15 parent metal.

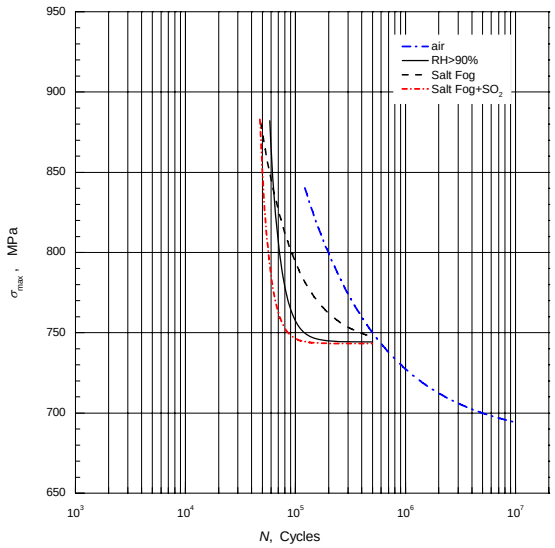

(a) R=0.5

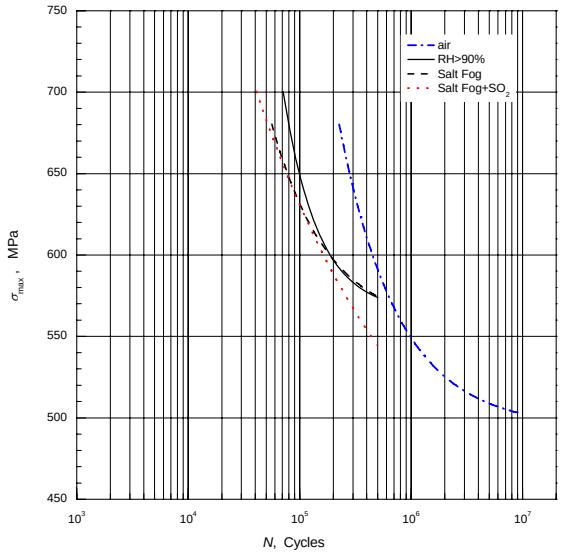

(b) R=0.06

Fig.8 Comparison among median fatigue S-N curves for welded joints in laboratory air and three kinds of corrosive environments (a) R=0.5, (b) R=0.06.

4. Fatigue Life Prediction and Verification

Based on a small crack methodology [3-4], the corresponding software, FASTRAN 3.9[5] was revised to predict the total fatigue life of two kinds of welded joints. The methodology is based on the plasticity-induced crack-closure concept and the effective stress intensity factor range, $\triangle K_{\text{eff}}$. The required elements for the fatigue life prediction are: crack shape and initial crack size, accurate stress intensity factor solutions of 3-D small cracks, and da/dN-$\triangle K_{\text{eff}}$ base-line data.

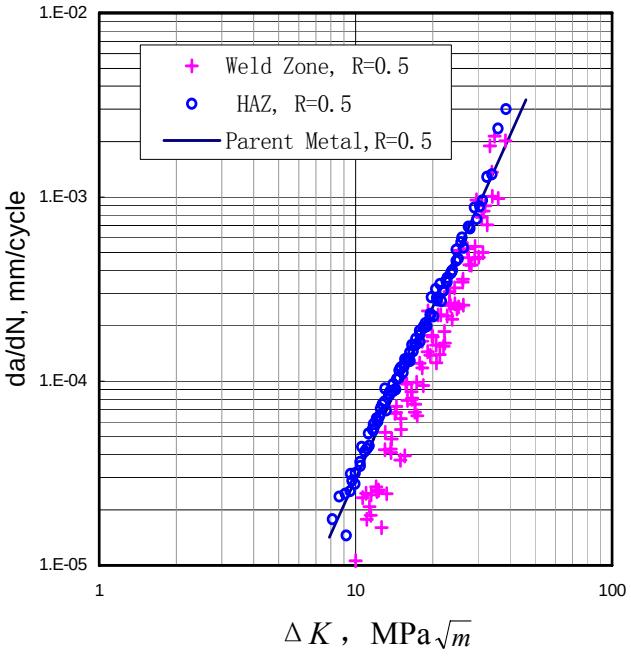

(a) R=0.5

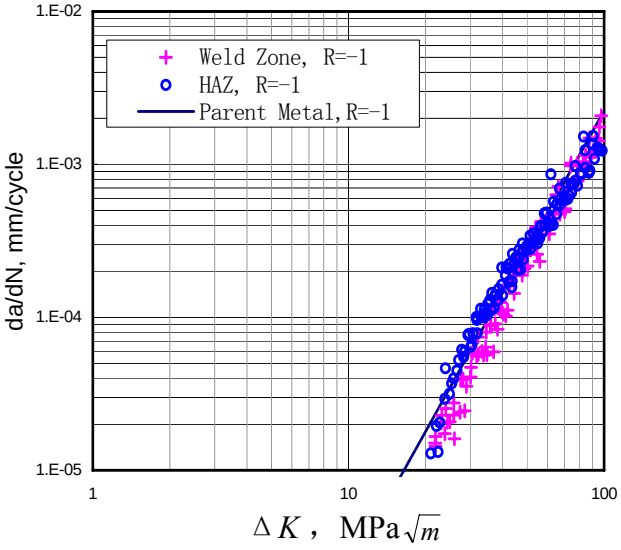

(b) R=-1

Fig 9 Comparison of large crack growth rates among the parent metal, welded zone and HAZ of argon-arc welded joint for different stress ratios at room temperature in laboratory air

By means of SEM fractographic analysis and measurements, most of defects were found to be subsurface porosities. The initial crack shape was treated as an embedded elliptical subsurface crack for stress intensity factor calculation. For the tension of finite thickness plates containing

an embedded elliptical crack located at an arbitrary position with one of its principal axes parallel to the plate surfaces, Isida and Noguchi[6] had proposed a stress intensity factor solution. This solution is added in the FRSTRAN3.9 code by the present authors.

Another important element for fatigue life prediction is the da/dN-$\triangle K_{eff}$ base-line curves of both argon-arc and electron-beam welded TA15 titanium alloys. Because most of cracks are initiated at the HAZ area, the da/dN-$\triangle K_{eff}$ curves for this area are determined by crack closure analyses based on the large crack growth data of the corresponding materials. Fig.10 showed da/dN vs. ΔK (or ΔK_{eff}) relationship at the HAZ for argon-arc welded joint at different stress ratios. The obtained da/dN-$\triangle K_{eff}$ baseline data is given in Table 3 for argon-arc and electron-beam welded joints, and shown in Fig.10 (b) for argon-arc welded joint. Considering that the large crack data for rates nearby the growth threshold may be influenced by closure due to the load-shedding procedure [3], the dashed line at the lower rate area in the Fig.10 (b) is estimated by trial-and-error to fit the endurance-limit behavior from the fatigue tests.

Table 3 Baseline data of crack growth for life prediction

Argon-arc welded joint		Electron-beam welded joint	
ΔK_{eff} [MPa.m$^{1/2}$]	da/dN [m/cycle]	ΔK_{eff} [MPa.m$^{1/2}$]	da/dN [m/cycle]
3.1	1E-11	3.1	1E-11
5	6E-10	4.6	1E-9
7.5	1E-8	5.8	1E-8
8	1.5E-8	6.4	2E-8
10	4.5E-8	7.8	5E-8
15	2.2E-7	10	1.2E-7
20	5E-7	19	1E-6
30	4E-6	30	6E-6
50	5E-5	50	8E-5

The fatigue-life prediction software based on small crack analysis, FASTRAN 3.9, was revised to predict the total fatigue lives for two kinds of TA15 titanium alloy welded joints. Careful SEM fractographic analyses for fractures of tested joints were carried out by Liu[1]. It was found that the size and location of the weld defect (porosity), from which a fatigue crack initiates and causes final failure of the welded joint, were different for various joints under different loading. The limited amount of data of the key weld defects from Reference[1] was used to verify the prediction. The sizes of the defects are from 0.076mm to 0.292mm. The distances to welded joint surface from the center of the weld defects are from 0.055mm to 1.212mm. Comparisons between the test and predicted lives are given in Figs.11 and 12 for argon-arc and electron-beam welded joints with various defects of different sizes and locations, respectively.

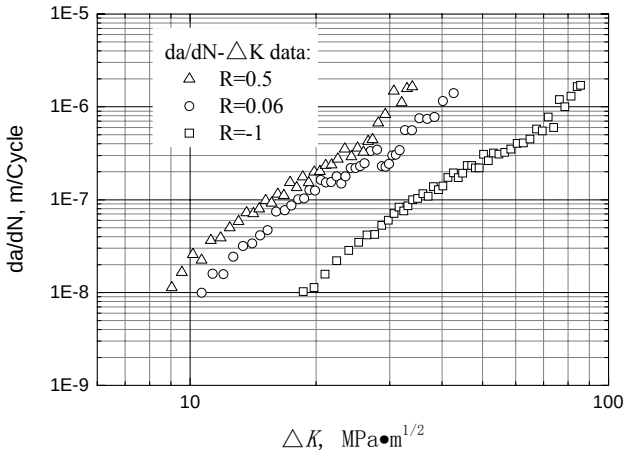

(a)

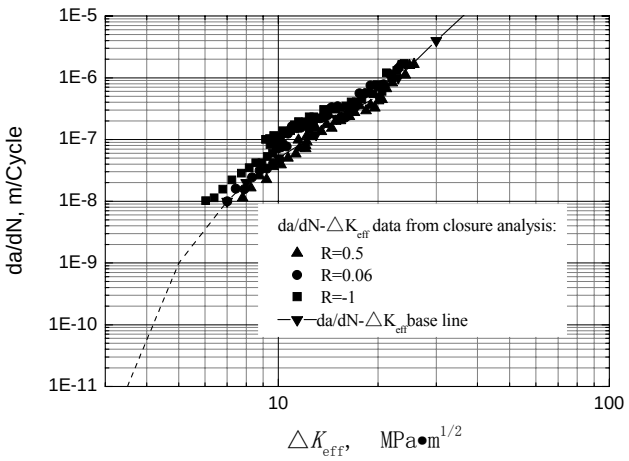

(b)

Fig.10 The da/dN vs. ΔK (or ΔK_{eff}) at the HAZ for argon-arc welded joint at different stress ratios

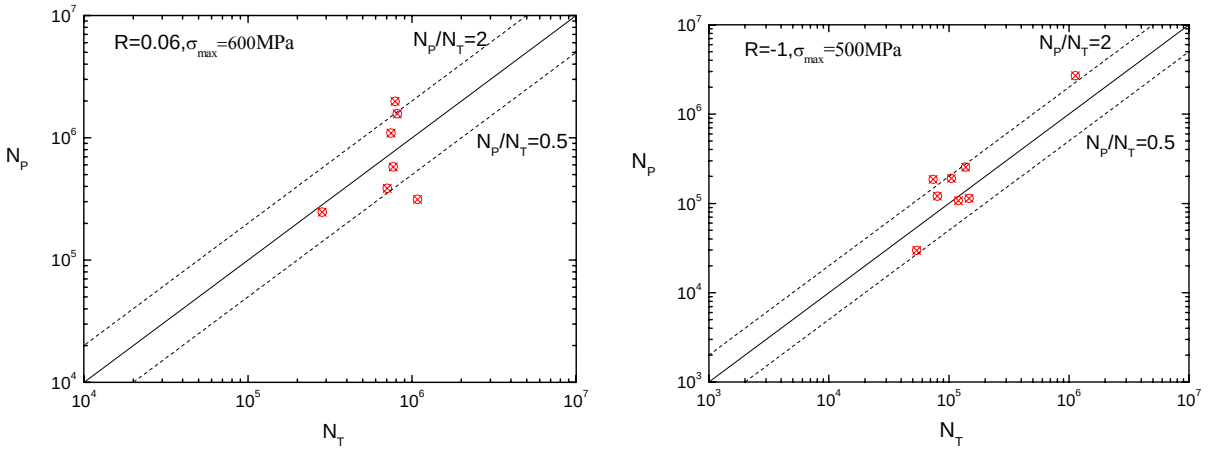

Fig.11 Comparison between the predicted and tested results for argon-arc welded joints with various weld defects of different sizes and locations at different loading stress ratios

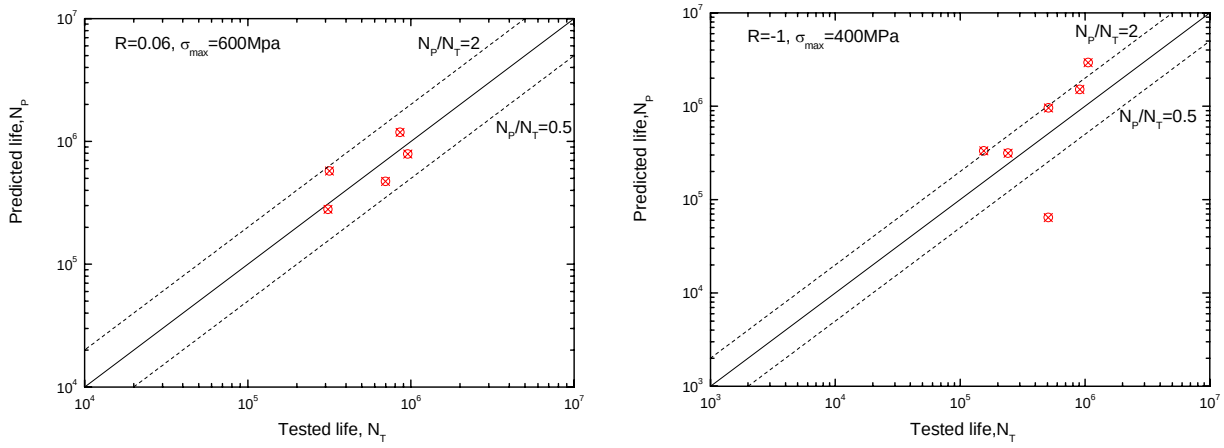

Fig.12 Comparison between the predicted and tested results for electron-beam welded joints with various defects of different sizes and locations at different stress ratios

5. Parametric Studies on Effect of Weld Defect on Fatigue Life

From Figs. 11 and 12, it can be found that the prediction agrees reasonably well with tests for all two kinds of welded joints with various defects at different loading stress ratios. Therefore, the revised software is used to simulate effect of the size and location of the weld defect on fatigue life of welded joint.

Parametric simulating studies can show the variation of the predicted fatigue life with weld defect size under the given distances from defect center to joint surface. And it can also show the variation of the predicted fatigue life with the distance from defect center to specimen surface under the given weld defect sizes.

The obtained results showed that the predicted life decreases as defect size increases under the given the distance to specimen surface, as shown in Fig.13 for electron-beam welded joint, and the predicted life becomes shorter when the weld defect is nearer to the specimen surface, as shown in Fig.14 for argon-arc welded joint. It can be also found that the effect of the distance from defect center to specimen surface on fatigue life becomes less obvious as the defect is farther from the specimen surface. The parametric studies showed that the effect of the size and location of weld defect on fatigue lives of two kinds of welded joints with different welded process is basically the same.

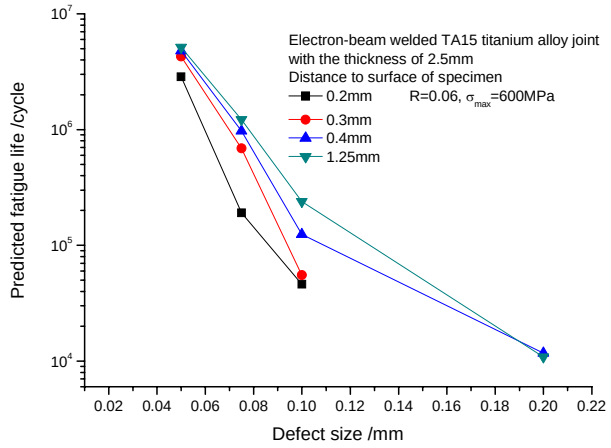

Fig.13 Variation of the predicted fatigue life with weld defect size for electron-beam welded joint

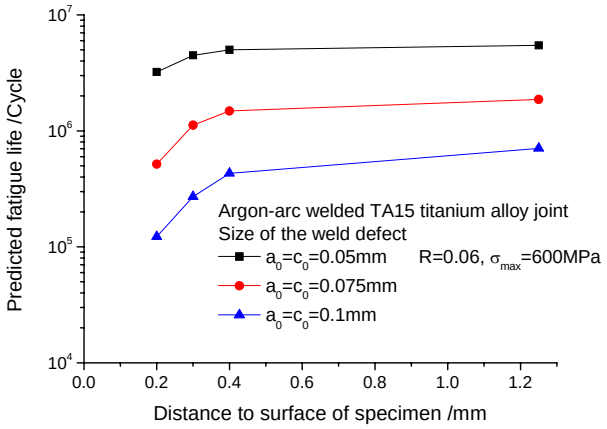

Fig.14 Variation of predicted fatigue life with the distance from defect center to specimen surface for argon-arc welded joint

6. Conclusions

(1) The fatigue properties of the parent metal are superior to those of the weld joints with two different welded processes at positive load ratios. An opposite tendency was found at a negative load ratio. Fatigue properties of weld joints are not much affected by different weld process, especially at or near fatigue limit.

(2) Large crack growth rates are higher for cracks in the HAZ than those of the weld zone and parent metal. The effect of temperature on large crack growth rates of the weld zone is not obvious. However, temperature effect on fatigue properties was found to be quite obvious. Fatigue properties of argon-arc welded joints in corrosive environment showed significant decrease when compared to those in laboratory air.

(3) Most of the fatigue cracks are initiated at weld porosities in the HAZ and at the edge of the weld. Nearly two-thirds of the specimens fractured near the HAZ. The size and location of the weld defect from which fatigue crack initiates and causes final failure are different for various specimens under different loadings.

(4) A revised FASTRAN3.9 code based on a small crack methodology was used to predict total fatigue lives of titanium alloy welded joints, and to study the effect of size and location of weld defect on fatigue lives of both electron-beam and argon-arc welded joints. Most of the predictions agreed reasonably well (within a factor of 2) with tests for different welded joints with various weld porosities of different sizes and locations. The effect of both the size and location of a weld defect on fatigue life is significant. The parametric studies found that the effect of the size and location of weld defect on fatigue lives of two kinds of welded joints with different welded process is basically the same.

References

[1] Liu C K. *Fatigue and fracture behavior of TA15 titanium alloy welded joint*, Master's Thesis, Beijing Institute of Aeronautical Materials, 2005 (in Chinese)

[2] Hu B R, and Liu J Z, et al. Fatigue behavior and life prediction for argon-arc weld joints based on small crack methodology, *Fracture and Strength of Solids VI*, pp157-162, 2006

[3] Wu X R, Newman J C Jr., et al. *Small crack effects in high-strength aluminum alloys — A NASA-CAE Fatigue and Fracture Mechanics Cooperative Program*, Aviation Industry Press, 1994

[4] Newman J C, Jr, Wu X R, et al. Small crack growth and fatigue life predictions for high-strength aluminum alloys: part II—crack closure and fatigue analyses, *Fatigue Fract Engng Mater Struct*, Vol.23, pp.59-72, 2000.

[5] Isisda M, Noguchi H. Tension of a plate containing an embedded elliptical crack, *Engng Fract. Mech.*, Vol.20, No.3, pp387-408, 1984.

[6] Newman J C Jr. FASTRAN II-A fatigue crack growth structural analysis program. *NASA TM-104159* , 1992.

Copyright Statement

The authors confirm that they, and/or their company or institution, hold copyright on all of the original material included in their paper. They also confirm they have obtained permission, from the copyright holder of any third party material included in their paper, to publish it as part of their paper. The authors grant full permission for the publication and distribution of their paper as part of the ICAS2008 proceedings or as individual off-prints from the proceedings.